Int. J. Electrochem. Sci., 15 **(2020)** 6060 – 6090, doi: 10.20964/2020.07.01

International Journal of
ELECTROCHEMICAL
SCIENCE
www.electrochemsci.org

Transport and kinetics in electrocatalytic thin film conducting polymer biosensors: bounded diffusion with Michaelis-Menten kinetics incorporating general inhibition effects

Michael EG Lyons

School of Chemistry and AMBER National Centre, University of Dublin, Trinity College Dublin, Dublin 2, Ireland.
E-mail: MELYONS@tcd.ie

Received: 4 March 2020 / *Accepted:* 26 April 2020 / *Published:* 10 June 2020

In this paper we discuss the problem of discussing the transport and catalytic reaction kinetics at redox enzymes immobilized within an electronically conductive polymer matrix where the effect of inhibition is specifically considered in the rate equation. Here the reaction kinetics are not of the simple Michaelis-Menten type. WE describe a mathematical procedure based on the recently developed technique developed by Akbari and Ganji which facilitates a full analytical solution of the boundary value problem which is valid over an extended substrate concentration range. Closed form expressions for both the substrate concentration in the film and the steady state amperometric current response are presented. 10 limiting kinetic cases are identified and discussed.

Keywords: Amperometric polymer sensor modelling; Michaelis-Menten kinetics with inhibition; Transport and kinetics in chemically modified electrodes; redox enzyme kinetics. Reaction/diffusion equations.

1. INTRODUCTION

The problem of quantitatively describing the transport and kinetics of reactants within bounded thin polymeric films (aka chemically modified electrodes) is very challenging and various approaches have been developed over the last 30 years[1.2]. The early work of Saveant et al[3] and Albery and Hillman[4] is seminal. This early work had a focus on describing diffusion coupled with bimolecular reaction or diffusion coupled with substrate pre-activation within a thin film. This topic remains of interest due to the fact that it enables the technologically important areas of chemical/bio-sensing and surface catalysis within fuel cell and electrolysis devices to be described in a mathematically precise manner[5,6]. Using this approach an analytical solution to a well defined reaction/diffusion problem can be developed which will describe how the concentration of the reactant (or substrate) will vary through

the catalytic layer as a function of distance and time. It also enables an expression for the net reaction rate or reaction flux to be derived. In electrochemical systems the reaction flux is usually expressed as a current. This can be related in a definite way to real system parameters such as catalyst loading, catalyst concentration, substrate concentration and film thickness. The mathematical model should make simple predictions on how the reaction rate depends on each of the latter parameters and thereby enable the rational design of a modified electrode in which substrate detection/catalysis is optimized. We have recently summarised advances in modelling the mechanism of mediated electron transfer at redox active surfaces where the binding interaction between surface site and substrate can be complex [7].

In the present paper we focus attention on amperometric chemical sensing via surface immobilized redox active catalytic species (such as redox enzymes) which are embedded in a polymeric support matrix. In amperometric detection the target analyte diffuses through the solution phase, partitions into the catalytic film, diffuses within the film and subsequently is oxidized at the catalyst surface within the layer . The oxidized active form of the reduced catalyst is regenerated via application of an oxidizing potential at the support electrode. Communication between the underlying support electrode is accomplished in one of two ways. If the matrix containing the catalytic species is electronically conductive then the active form of the catalyst may be regenerated at a polymer strand which is in direct electronic communication with the support electrode surface and hence responds the applied potential input. Conversely if the polymer matrix in non conducting a small molecule redox mediator may be used to shuttle charge between catalyst and support electrode thus facilitating catalyst regeneration and turnover. The redox mediator (in its reduced form) diffuses from the solution, partitions into the film, diffuses to the catalytic site, reacts there and subsequently a fraction of the oxidized mediator diffuses to the electrode where it is regenerated via oxidation to its reduced form to continue the catalytic cycle. Some oxidized mediator diffuses in the opposite direction and is lost from the layer. In this paper we only consider the first scenario in which the polymer matrix is electronically conducting[8]. This scenario is presented in fig.1. The second scenatio, that of a non conducting polymer matrix with charge shuttling between enzyme active site and underlying support electrode, has been previously described[9].

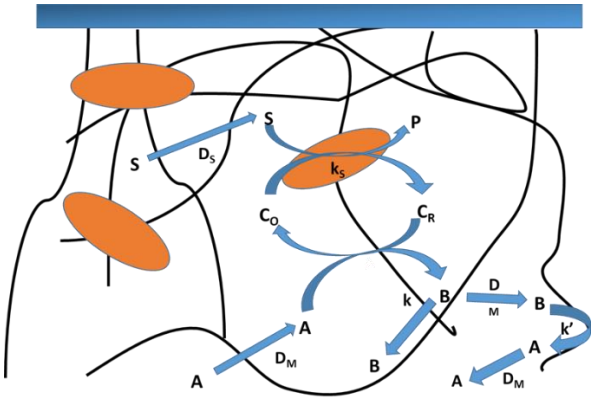

Figure 1. Schematic representation of reaction/diffusion in a conducting polymer matrix containing immobilized catalytic particles such as redox enzymes. The polymer strand serves as a molecular wire and the mediator reacts along the polymer strand.

Consequently we focus attention on the situation where the redox enzyme is immobilized within an electronically conducting polymer material[8]. We assume planar diffusion of substrate within a conductive film of thickness L. Substrate diffusion within the film obeys the Fick diffusion equation. Furthermore, we assume that the substrate/enzyme reaction exhibits Michaelis-Menten kinetics. We will extend our previously published analysis[8] and solve the relevant reaction/diffusion equation to obtain a useful closed form analytical expression for the substrate concentration profile within the thin film (i) when inhibition effects are initially absent and (ii) when they operate. We well then derive an expression for the steady state amperometric current response.

The reaction diffusion equation pertinent to this problem will be non-linear because of the Michaelis-Menten kinetic term. In recent years Rajendran and co-workers[10.11] have used the variational iteration method (VIM) to model the response of a potentiometric and amperometric enzyme sensor in which linear diffusion is coupled to non linear Michaelis-Menten kinetics. This technique produces solutions to the boundary value problem in terms of convergent series requiring no linearization or small perturbation. The analytical results valid for all saturation parameter values were compared with those earlier limiting cases proposed by Lyons et al[8] and were found to be in good agreement. More recently Malvandi and Ganji[12] developed a variational iteration method coupled with Padé approximation (VIM-Padé) to obtain analytical expressions involving rational functions for substrate concentration profiles for bounded catalytic systems with non linear Michaelis-Menten Kinetics. Rajendran et al[13-15] outlined how the method of homotopy perturbation could be used to derive an analytical expression for the substrate concentration profile within a thin layer when the reaction kinetics exhibit Michaelis-Menten kinetics. Finally Dharmalingam and Veeramuni[16] applied the Akbari-Ganji method (AGM) to develop an expression for the amperometric current response to non linear reaction/diffusion in an electroactive polymer film.

It has long been recognised that enzyme reaction kinetics may be affected by the presence of an inhibitor . Enzyme function can be affected by substances called inhibitors (which we denote as I). Often, a reversible association of inhibitor with enzyme E prevents product P formation. Hence, either the enzyme/inhibitor complex EI is incapable of binding substrate S, or if the substrate is bound, it cannot react to form product. In this paper attention will be focused on the manner in which mixed inhibition (MI) can be factored into a reaction/diffusion equation involving Michaelis-Menten reaction kinetics in a bounded diffusion region (a thin polymeric film). In mixed inhibition the inhibitor I may bind to the enzyme whether or not the latter has already bound the substrate S, but has a greater affinity for one state or the other. Mixed Inhibition is a conceptual mixture of competitive inhibition (CI) in which the inhibitor I can only bind to the catalytic site if the substrate S has not already bound, and uncompetitive inhibition (UI) in which I can only bind with the enzyme if the substrate S has already been bound. If the ability of I to bind with the catalyst is exactly the same whether or not the catalyst is already bound to substrate, it is known as non competitive inhibition (NCI). We have already discussed the interesting case of substrate inhibition (SI) in a recent paper[17]. Albery and co-workers[18] have also made a seminal contribution to the problem of enzyme kinetics in bounded regions with product inhibition operating.

2. PLANAR REACTION DIFFUSION IN A BOUNDED REGION.

2.1. Inhibition Effects Absent

We initially consider the simple case of planar diffusion and reaction of substrate S within a thin conductive film of thickness L immobilized on a support electrode containing a homogeneous distribution of catalytic enzyme particles of concentration e_Σ . The enzyme particle are assumed to be immobile. Hence the governing reaction diffusion equation admits the following form:

$$D_S \frac{\mathrm{d}^2 s}{\mathrm{d}x^2} - \frac{k_c e_\Sigma s}{K_M + s} = 0 \tag{4}$$

In this expression we introduce the pseudo first order rate constant $k = k_c e_\Sigma / K_M$ where e_Σ denotes the total catalyst concentration (molcm^{-3}) respectively. This equation must be solved subject to the following boundary conditions:

$$x = 0 \quad \frac{\mathrm{d}s}{\mathrm{d}x} = 0 \quad x = L \quad s = \kappa s^\infty \tag{5}$$

Here κ denotes the partition coefficient of substrate and s^∞ is the bulk concentration of substrate in solution. Hence the product κs^∞ represents the reactant concentration at the layer solution interface. The latter boundary condition implicitly assumes that concentration polarization of substrate in the solution may be neglected.

We introduce the following dimensionless quantities:

$$u = \frac{s}{\kappa s^\infty} \quad \chi = \frac{x}{L} \quad \alpha = \frac{\kappa s^\infty}{K_M} \quad \gamma = \Phi^2 = \frac{kL^2}{D_S} \tag{6}$$

Where u, χ represent the dimensionless concentration and distance parameters respectively. Furthermore α denotes a saturation parameter and γ defines a reaction/diffusion parameter. The saturation parameter compares the value of the substrate concentration in the layer to the Michaelis constant. When this parameter is small the catalytic kinetics is unsaturated and the rate is first order with respect to substrate concentration. When it is large the kinetics are saturated and zero order kinetics pertain. The reaction /diffusion parameter compares the rate of reaction between substrate and catalyst moiety and the rate of substrate diffusion in the layer and is directly related to the Thiele modulus via the following expression: $\sqrt{\gamma} = \Phi = L / X_K$ where $X_K = \sqrt{D_S / k}$ denotes a characteristic reaction layer thickness which is a measure of the distance travelled by the substrate in the film before it reacts with the immobilized catalyst particle.

Hence eqn.4 transforms to:

$$\frac{\mathrm{d}^2 u}{\mathrm{d}\chi^2} - \frac{\gamma u}{1 + \alpha u} = 0 \tag{7}$$

which must satisfy the following boundary conditions

$$\begin{aligned} &\chi = 0 \quad u = u_0 \quad \frac{\mathrm{d}u}{\mathrm{d}\chi} = 0 \\ &\chi = 1 \quad u = 1 \end{aligned} \tag{8}$$

Now the net amperometric current corresponding to the rate of substrate reaction in the layer is given by the following equivalent expressions:

$$i = nFAD_S\left(\frac{ds}{dx}\right)_{x=L} = \frac{nFA(k_c / K_M)e_\Sigma}{1+\kappa s^\infty / K_M}\int_0^L s(x)dx \qquad (9)$$

Consequently we can introduce a normalised steady state current or reaction flux y as follows:

$$y = \frac{iL}{nFAK_M D_S} = \alpha\left(\frac{\mathrm{d}u}{\mathrm{d}\chi}\right)_{\chi=1} = \frac{\alpha\gamma}{1+\alpha}\int_0^1 u(\chi)\,d\chi \qquad (10)$$

Hence the problem reduces to evaluating an analytical expression for u which will be valid for all values of γ and α . Once this is achieved an analytical expression for the normalised flux of the amperometric sensor can be readily derived via eqn.10.

In earlier work[8] we have proposed analytical steady state solutions to eqn.9 which are valid for the limiting cases of low and high saturation parameter values, and have proposed a solution based on the reasonable assumption that the non - linear kinetic term $\frac{u}{1+\alpha u}$ can be approximated by the linear expression $\frac{\alpha+u}{(1+\alpha)^2}$. Hence the reaction/diffusion equation transforms to:

$$\frac{\mathrm{d}^2u}{\mathrm{d}\chi^2} - \frac{\gamma(\alpha+u)}{(1+\alpha)^2} = 0 \qquad (11)$$

We have shown that this approximation is valid only for certain values of α and u. Specifically the approximation pertains for all values of u where the Michaelis-Menten kinetics are unsaturated (when $\alpha < 1$. For $\alpha > 1$ the approximation becomes inaccurate if significant depletion of substrate occurs within the film , if u falls to less than 0.8 at any point in the film. This will occur when the parameter γ is large. In short our strategy was to transform the non linear reaction/diffusion equation into a linear equation which can be readily integrated.

In this paper we further develop the AGM to examine steady state non linear reaction diffusion in bounded thin films of planar slab geometry with a particular focus on amperometric detection. Hence we solve eqn.7 subject to the conditions outlined in eqn.8 to obtain approximate closed form analytical expressions for the substrate concentration profile and the normalised reaction flux which are valid for all values of the saturation parameter α and defined values of the reaction diffusion parameter γ . We will compare the approximate solution with the numerical solution obtained using the NDSolve facility in Mathematica 12 to determine the parameter set where goodness of fit between the simulated and closed analytical solution is optimized. We do this for the slab geometry. The cases of both spherical and cylindrical diffusion coupled with non linear Michaelis-Menten reaction kinetics will be discussed in a subsequent paper .

We follow the recent excellent work of Dharmalingam and Veeramuni[15] and assume that a suitable solution for the reaction/diffusion presented in eqn. 7 will have the following form:

$$u(\chi) = A\cosh[\beta\chi] + B\sinh[\beta\chi] \qquad (12)$$

We can readily show using the boundary conditions presented in eqn.8 that $A = \operatorname{sech}\beta$ and $B = 0$ and we obtain:

$$u(\chi) = \frac{\cosh[\beta\chi]}{\cosh[\beta]} \qquad (13)$$

We now use the approach of Dharmalingam and Veeramuni[15] and we use the Akbari-Ganji method (AGM) to evaluate the unknown parameter β . This is a powerful semi-analytic approach for solving non linear ordinary differential equations. In this method a solution function consisting of unknown constant coefficients is assumed satisfying the target differential equation. This solution is substituted into the latter to generate one or more algebraic equations. Finally, the unknown coefficients are computed using these algebraic equations in which a relevant boundary condition is inserted . The literature describing this method is not at all clear in discussing the general validity of this approach. However the closed form approximate analytical solutions obtained using AGM are in good agreement with numerically simulated results and with other approximate methods of solution such as VIM or HPM[9,10,12-14]. To follow AGM we introduce the following function:

$$f(u'',u,\chi)=\frac{\mathrm{d}^2u}{\mathrm{d}\chi^2}-\frac{\gamma u}{1+\alpha u}=0 \tag{14}$$

Hence substituting eqn.13 into eqn.14 we obtain:

$$f(u'',u,\chi)=\beta^2\,\mathrm{sech}\,\beta\cosh\left[\beta\chi\right]-\frac{\gamma\,\mathrm{sech}\,\beta\cosh\left[\beta\chi\right]}{1+\alpha\,\mathrm{sech}\,\beta\cosh\left[\beta\chi\right]} \tag{15}$$

This will only be true provided $\chi=1$ [1] and so from eqn.8 we note that:

$$f(\chi=1)=\beta^2-\frac{\gamma}{1+\alpha}=0 \tag{16}$$

Consequently we obtain t:

$$\beta=\sqrt{\frac{\gamma}{1+\alpha}} \tag{17}$$

Hence the solution to eqn.6 is:

$$u(\chi)=\frac{\cosh\left[\sqrt{\frac{\gamma}{1+\alpha}}\chi\right]}{\cosh\left[\sqrt{\frac{\gamma}{1+\alpha}}\right]} \tag{18}$$

Furthermore the substrate concentration at $\chi=0$ is given by: $u_0=\mathrm{sech}\left[\sqrt{\frac{\gamma}{1+\alpha}}\right]$.

The very interesting result presented in eqn.18 can also be obtained by employing the Homotopy Perturbation method (HPM)[19,20].

We again consider eqn.7 and the boundary conditions outlined in eqn.8. We can construct the following homotopy:

$$(1-p)\left\{\frac{\mathrm{d}^2u}{\mathrm{d}\chi^2}-\frac{\gamma u}{1+\alpha u_1}\right\}+p\left\{(1+\alpha u)\frac{\mathrm{d}^2u}{\mathrm{d}\chi^2}-\gamma u\right\}=0 \tag{19}$$

[1] The fact that we need to evaluate the substrate concentration gradient at $\chi=1$ using this expression for the substrate concentration suggests that the expression derived for the normalized current is validly obtained.

Here p is an embedding parameter and $p \in [0,1]$. Taking the limit as $p \to 0$ we obtain the zeroth order approximation[2]:

$$\frac{\mathrm{d}^2 u}{\mathrm{d}\chi^2} - \frac{\gamma u}{1+\alpha} = 0 \tag{20}$$

This is valid since $u_1 = 1$ from eqn.8. This expression has the solution given by eqn.18 with

$$u_0 = \operatorname{sech}\left[\sqrt{\frac{\gamma}{1+\alpha}}\right]$$

When we have unsaturated catalytic kinetics and $\alpha << 1$, then eqn.18 reduces to:

$$u(\chi) \cong \operatorname{sech}\left[\sqrt{\gamma}\right]\cosh\left[\sqrt{\gamma}\chi\right] \tag{21}$$

This is the same as eqn.10 in our initial 1996 paper [8]. Alternatively for saturated catalytic kinetics $\alpha >> 1$ and eqn.18 reduces to:

$$u(\chi) \cong \operatorname{sech}\left[\sqrt{\frac{\gamma}{\alpha}}\right]\cosh\left[\sqrt{\frac{\gamma}{\alpha}}\chi\right] \tag{22}$$

Eqn.22 can be simplified further. If the argument in the hyperbolic cosine functions is small then we can Taylor expand the functions to give: $\cosh\left[\sqrt{\frac{\gamma}{\alpha}}\chi\right] \cong 1 + \frac{\gamma}{2\alpha}\chi^2$ and $\operatorname{sech}\left[\sqrt{\frac{\gamma}{\alpha}}\right] \cong 1 - \frac{\gamma}{2\alpha}$ and so the substrate concentration profile when the catalytic kinetics are saturated is alternatively given by:

$$u(\chi) \cong \left(1 - \frac{\gamma}{2\alpha}\right)\left(1 + \frac{\gamma}{2\alpha}\chi^2\right) = 1 - \frac{\gamma}{2\alpha}\left(1 - \left(1 - \frac{\gamma}{2\alpha}\right)\chi^2\right) \tag{23}$$

This expression for the concentration profile is valid when $\frac{\gamma}{2\alpha} < 1$. The expression in eqn.23 is the same as that presented in eqn.11 of our initial 1996 paper[8].

When the reaction/diffusion parameter γ is large then the catalytic reaction kinetics are much faster than substrate diffusion through the film, then we note that $\cosh\left[\sqrt{\frac{\gamma}{1+\alpha}}\chi\right] \cong \frac{1}{2}\exp\left[\sqrt{\frac{\gamma}{1+\alpha}}\chi\right]$ and $\operatorname{sech}\sqrt{\frac{\gamma}{1+\alpha}} \cong 2\exp\left[-\sqrt{\frac{\gamma}{1+\alpha}}\right]$ and so the normalised substrate concentration profile takes the following form:

$$u(\chi) \cong \exp\left[-\sqrt{\frac{\gamma}{1+\alpha}}(1-\chi)\right] \tag{24}$$

Physically this expression corresponds to an exponential decay in concentration from an initial value of u = 1 at $\chi = 1$ with a time constant of $\sqrt{\frac{\gamma}{1+\alpha}}$ in a direction going in to the film from the outer

---

[2] We can show that the first order approximation to the substrate concentration in the film, which we label $u^{(1)}$, is given by: $\frac{\mathrm{d}^2 u^{(1)}}{\mathrm{d}\chi^2} - \frac{\gamma u^{(1)}}{1+\alpha} + \frac{\gamma u^{(0)}}{1+\alpha} - \frac{\gamma u^{(1)}}{1+\alpha u^{(1)}} = 0$ where $u^{(0)}$ is given by eqn.18. Hence a more accurate solution to the boundary value problem is: $u(\chi) = u^{(0)} + pu^{(1)} + \ldots\ldots$.

surface. Hence there is considerable concentration polarization of substrate in the layer. Alternatively when the reaction/diffusion parameter is small corresponding to the case where catalytic reaction kinetics are more sluggish than substrate diffusion through the layer corresponding to for $\gamma << 1$ we note that :

$$u(\chi) = \operatorname{sech}\left[\sqrt{\frac{\gamma}{1+\alpha}}\right]\cosh\left[\sqrt{\frac{\gamma}{1+\alpha}}\chi\right] \cong \left(1-\frac{\gamma}{2(1+\alpha)}\right)\left(1+\frac{\gamma}{2(1+\alpha)}\chi^2\right) \cong 1 \qquad (25)$$

Hence under these circumstances there is little concentration polarization of substrate within the film. The unsaturated catalytic kinetics are much more sluggish than substrate diffusion, and a uniform substrate concentration with little depletion is expected in the layer.

The approximate analytical solution outlined in eqn.18 is directly compared with the numerical integration of the non-linear reaction/diffusion equation presented in eqn.7. This was achieved using the NDSolve capability in Mathematica 12. The results are presented in fig.2 for the case of unsaturated catalytic kinetics and in fig.3 for saturated catalytic kinetics. We note that the correspondence between simulated and closed form analytical solutions are generally excellent in both scenarios. In fig.4 we examine the general case where the saturation parameter is close to unity. Here we choose $\alpha = 1$ an compare simulation results with the closed form analytical solution under conditions where the balance between catalytic kinetics and substrate diffusion is varied. Again very good agreement is observed . The largest divergence is observed in panel C where substrate depletion is significant which occurs at large γ values. These results suggest that the general solution is of most use is the scenario where there is balance between catalytic reaction kinetics and substrate diffusion and where the substrate concentration in the film is close to the Michaelis constant of the catalytic reaction.

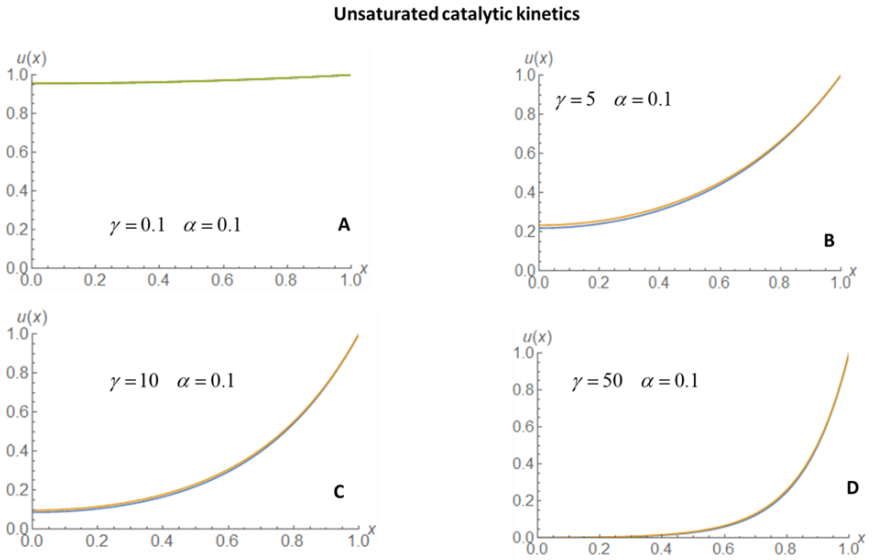

Figure 2. The variation of substrate concentration within the layer under conditions of unsaturated catalytic kinetics ($\alpha << 1$). The numerical solution (blue curve) is compared with eqn.18 (orange curve). The substrate diffusion rate as compared with the rate of catalytic reaction increases from panel A through panel D.

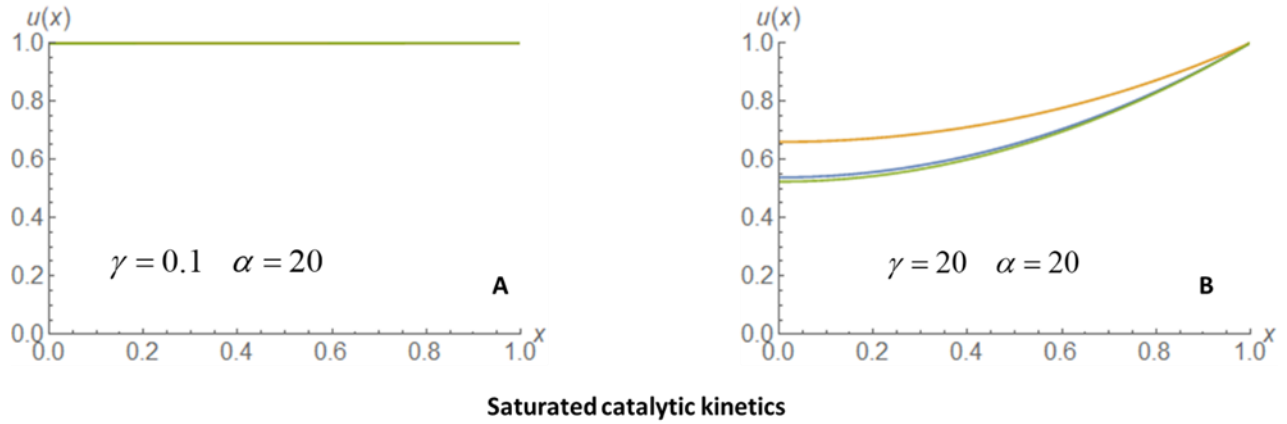

Figure 3. The variation of substrate concentration within the layer under conditions where the catalytic kinetics are saturated ($\alpha = 20$). In panel A the catalytic kinetics are much slower than substrate diffusion, whereas in panel B substrate diffusion is much slower than the catalytic kinetics and substrate depletion is significant. Here the best fit with the simulation (blue curve) is the profile corresponding to eqn.23 (green curve) rather than that predicted from eqn.18 (orange curve).

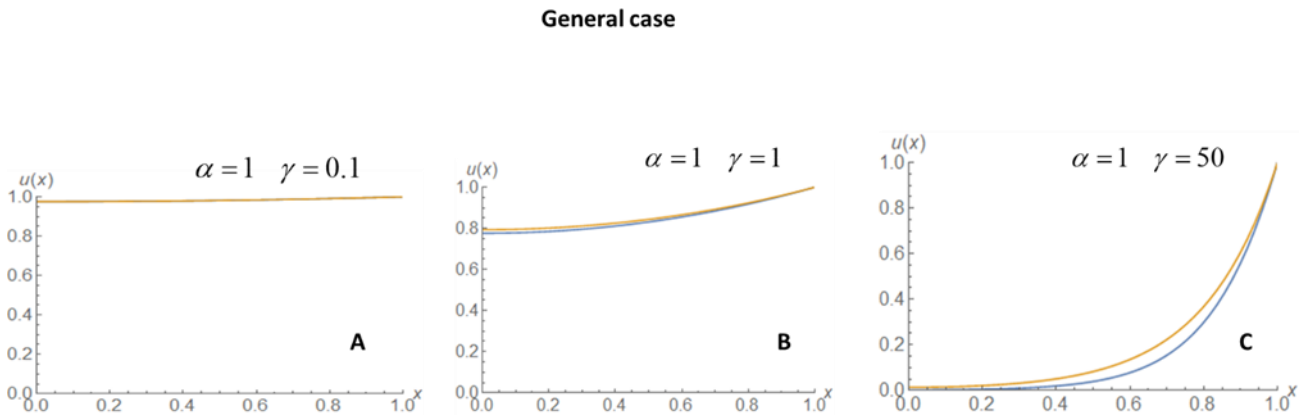

Figure 4. The variation of substrate concentration within the layer under conditions where the catalytic kinetics are borderline between unsaturated and saturated ($\alpha = 1$). In panel A the catalytic kinetics are much slower than substrate diffusion, whereas in panel B catalytic kinetics and substrate diffusion are in balance. In panel C substrate diffusion is much slower than the catalytic kinetics and substrate depletion is significant. The numerical solution (blue curve) and the closed form analytical solution (orange curve) are in very good agreement except when substrate depletion within the layer is significant (large γ values).

The normalised current response y is obtained via eqn.10 . We may readily show that:

$$y = \alpha \left(\frac{du}{d\chi} \right)_{\chi=1} = \alpha \sqrt{\frac{\gamma}{1+\alpha}} \tanh \left[\sqrt{\frac{\gamma}{1+\alpha}} \right] \tag{26}$$

This expression is termed the general case and will pertain to the situation where the catalytic kinetics are neither unsaturated nor saturated when α is close to unity. In fig. 5 the variation of the normalised current computed via eqn.26, with saturation parameter α, is presented for values of the

reaction/diffusion parameter γ in the range 0.05 to 15. This is in effect a normalised calibration curve , which depicts the variation of current response with substrate concentration. In fig. 6 the normalised current is plotted as a function of reaction/diffusion parameter γ , for various defined values of the saturation parameter ranging from 0.1 to 10. Limiting values for the normalised amperometric current response valid for all γ values are readily derived in the limits of: $\alpha << 1$ and $\alpha >> 1$ respectively. Furthermore other limiting expressions are obtained in the limit of $\gamma << 1$ and $\gamma >> 1$ for all α values. Eqn. 26 defines the general case.

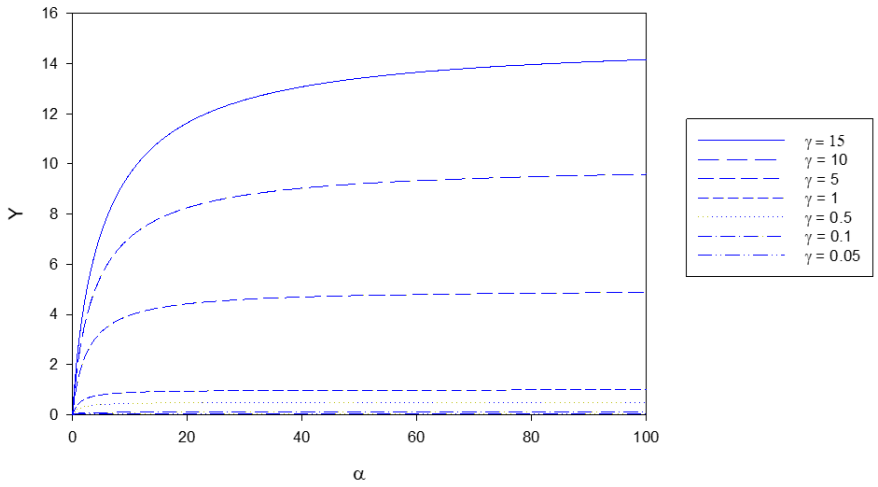

Figure 5. The variation of normalised current with saturation parameter computed via eqn.26. This defines the calibration curve for an amperometric sensor exhibiting Michaelis-Menten kinetics.

In our earlier 1996 paper[8] we quoted an empirical expression constructed by Albery and co-workers[16] for immobilized enzyme electrodes which could be adapted to describe reaction/diffusion in electroactive thin films. Indeed we fitted our experimental data to this expression. The Albery equation is :

$$y_A = \sqrt{2\gamma\left(\alpha - \ln\left(1+\alpha\right)\right)}\tanh\left[\frac{\alpha\sqrt{\gamma}}{\left(1+\alpha\right)\sqrt{2\left(\alpha-\ln\alpha\right)}}\right] \qquad (27)$$

In fig.7 we compare eqn.24 and eqn.25 derived using AGM proposed by Dharmalingam and Veeramuni[16] directly for a fixed value of $\gamma = 15$ and for a range of saturation parameter values between 0 and 100. Both normalised current response curves exhibit a similar development but the Albery expression over estimates the normalised flux by a significant amount.

In fig.8 we present the variation of the steady state flux ratio $Y = y/y_A$ as a function of saturation parameter α values over a wide range from 0 to 1000. Each curve presented corresponds to a set value of the reaction/diffusion parameter γ ranging from 0.1 to 1000. This figure suggests that when γ values are less than 0.1 the normalised flux ratio is essentially unity over the entire range of α values. However as the magnitude of γ increases corresponding to more favourable catalytic reaction kinetics in the layer, the normalised flux ratio Y initially decreases with increase in α value, to a broad minimum located within a specific α value range, and then increases again as the saturation parameter value is increased still further to approach a value of unity in the limit of large saturation parameter values. Furthermore,

the location of the flux ratio minimum varies with γ value, being located at increasingly larger α values as the catalytic kinetics become more rapid.

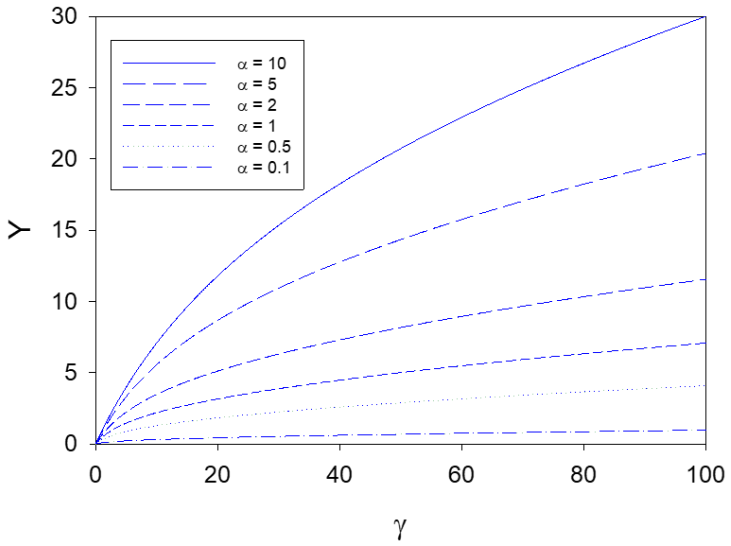

Figure 6. Variation of normalised current response computed via eqn.26 with reaction/diffusion parameter for various values of saturation parameter.

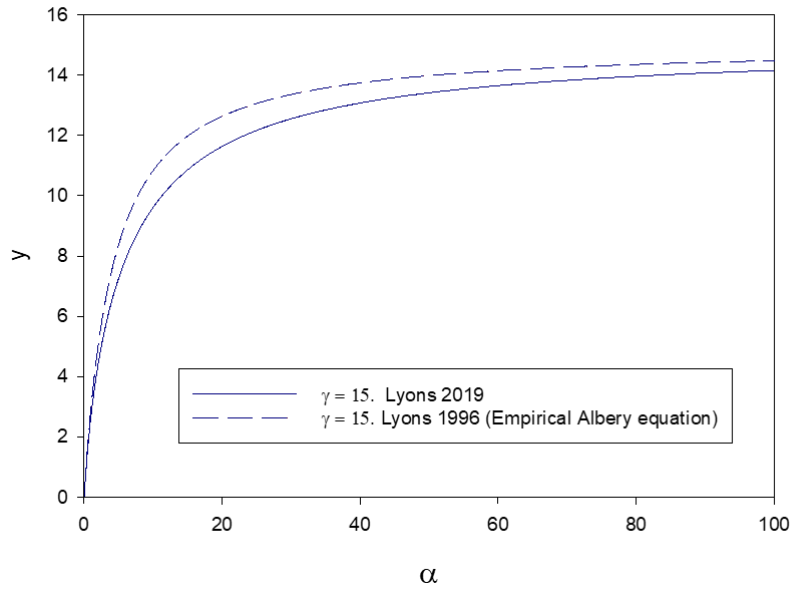

Figure 7. The expression derived by Albery (eqn.27) and the expression presented in the current work derived from AGM or indeed via HPM (eqn.26) for the normalised flux compared for a fixed value of reaction/diffusion parameter $\gamma = 15$.

So the prediction of normalised current according to Albery (eqn.27) and the present work (eqn.26) are very similar when the catalytic kinetics are sluggish over a wide range of substrate

concentration, but when the kinetics are more rapid the Albery expression over predicts the normalised flux by a factor of 20-35% over a significant range of α values.

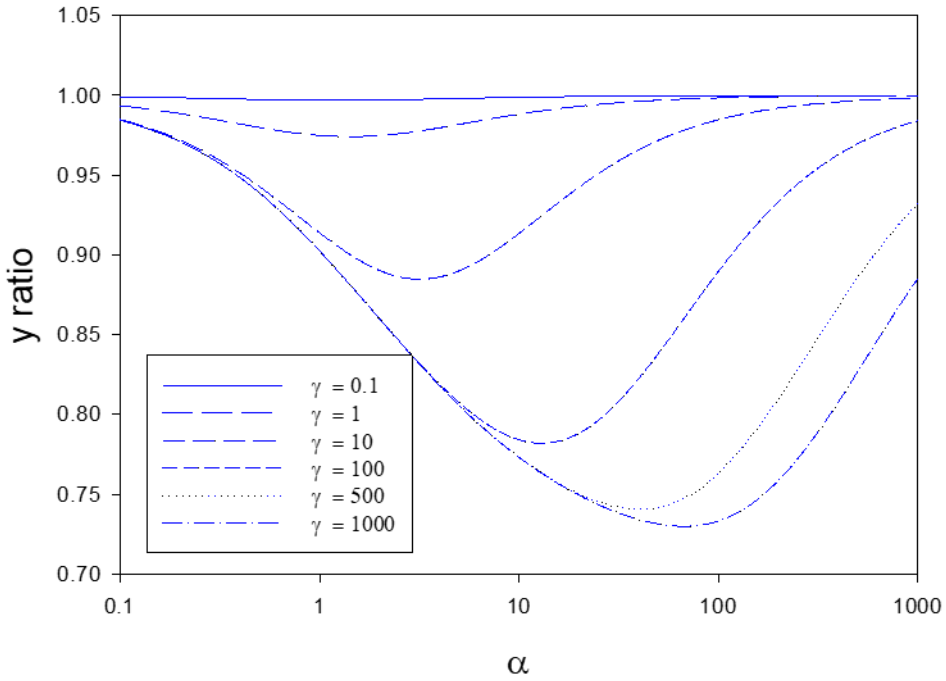

Figure 8. The variation of the normalised flux ratio with saturation parameter. Curves have been computed for various values of the reaction/diffusion parameter.

Following on from our previous paper[8] we note that eqn.7 can be written as:

$$\frac{\mathrm{d}u}{\mathrm{d}\chi}\left\{\frac{\mathrm{d}^2u}{\mathrm{d}\chi^2}\right\}=\gamma\frac{\mathrm{d}u}{\mathrm{d}\chi}\left\{\frac{u}{1+\alpha u}\right\} \tag{28}$$

Also we note that:

$$\frac{\mathrm{d}}{\mathrm{d}\chi}\left\{\frac{\mathrm{d}u}{\mathrm{d}\chi}\right\}^2=2\left(\frac{\mathrm{d}u}{\mathrm{d}\chi}\right)\frac{\mathrm{d}^2u}{\mathrm{d}\chi^2} \tag{29}$$

Hence we obtain:

$$\begin{aligned}\frac{\mathrm{d}}{\mathrm{d}\chi}\left\{\frac{\mathrm{d}u}{\mathrm{d}\chi}\right\}^2&=2\gamma\left\{\frac{u}{1+\alpha u}\right\}\frac{\mathrm{d}u}{\mathrm{d}\chi}\\ d\left\{\frac{\mathrm{d}u}{\mathrm{d}\chi}\right\}^2&=2\gamma\left\{\frac{u}{1+\alpha u}\right\}\mathrm{d}u\end{aligned} \tag{30}$$

Integrating we get:

$$\left\{\frac{\mathrm{d}u}{\mathrm{d}\chi}\right\}^2=2\gamma\int_0^u\frac{u\,\mathrm{d}u}{1+\alpha u}=2\gamma\left\{\frac{u}{\alpha}-\frac{1}{\alpha^2}\ln\left(1+\alpha u\right)\right\} \tag{31}$$

Hence the normalised current is given by:

$$y=\alpha\left(\frac{\mathrm{d}u}{\mathrm{d}\chi}\right)_{\chi=1}=\sqrt{2\alpha^2\gamma\left\{\frac{1}{\alpha}-\frac{1}{\alpha^2}\ln\left(1+\alpha\right)\right\}}=\sqrt{2\gamma\left\{\alpha-\ln\left(1+\alpha\right)\right\}} \tag{32}$$

Here we have assumed that $\mathrm{d}u/\mathrm{d}\chi = 0$ when $u = 0$ and $u = 1$ when $\chi = 1$. This expression for the normalised current is valid under conditions where $\alpha \cong 1$ and for large γ [3] . This expression corresponds to the situation where the inner region of the film is unsaturated whereas the outer region is saturated. We have shown previously[8] that the line of demarcation between these two regions is set at some critical distance $\chi^* = 1 - \sqrt{\frac{2\alpha}{\gamma}}$. Complete saturation occurs when $\chi^* = 0$. This is the two region scenario.

As previously noted[8] we can identify four limiting cases of eqn.26 and also of eqn.27. The behaviour of the system can be well described in terms of a kinetic case diagram which is a plot of $\log\gamma$ versus $\log\alpha$. This case diagram is outlined in fig .9. One limiting case arises when the catalytic kinetics are saturated. Hence $\alpha << 1 \quad \forall\gamma$ and we note that the normalised flux reduces to:

$$y \cong \alpha\sqrt{\gamma}\tanh[\gamma] \tag{33}$$

This expression combines two limiting cases. Case I pertains when the catalytic kinetics are slower than substrate diffusion and $\gamma << 1$. Hence $\tanh\sqrt{\gamma} \cong \sqrt{\gamma}$ and eqn.33 reduces to:

$$y \cong \alpha\gamma \tag{34}$$

Translating back into dimensioned quantities we obtain:

$$i = nFA(k_c/K_M)e_\Sigma L\kappa s^\infty \tag{35}$$

Hence the amperometric current response is first order with respect to substrate concentration, catalyst concentration, and layer thickness. The reaction occurs uniformly throughout the film. On the other hand when $\gamma >> 1$ the reaction kinetics are rapid and we note that $\tanh\sqrt{\gamma} \cong 1$ and eqn.33 reduces to:

$$y \cong \alpha\sqrt{\gamma} \tag{36}$$

This corresponds to case II. Under these circumstances $L >> X_K$ the layer thickness is much greater than the kinetic length and so reaction occurs in a thin reaction layer at the outside of the film. This will pertain when the reaction kinetics between substrate and catalytic sites occur rapidly. Hence the current response is given by:

$$i = nFA(k_c/K_M)e_\Sigma X_K\kappa s^\infty = nFA\sqrt{\frac{k_c D_S}{K_M}}e_\Sigma^{1/2}\kappa s^\infty \tag{37}$$

[3] Specifically this solution will be valid when $\alpha > 1$ but $\alpha < \gamma/2$.

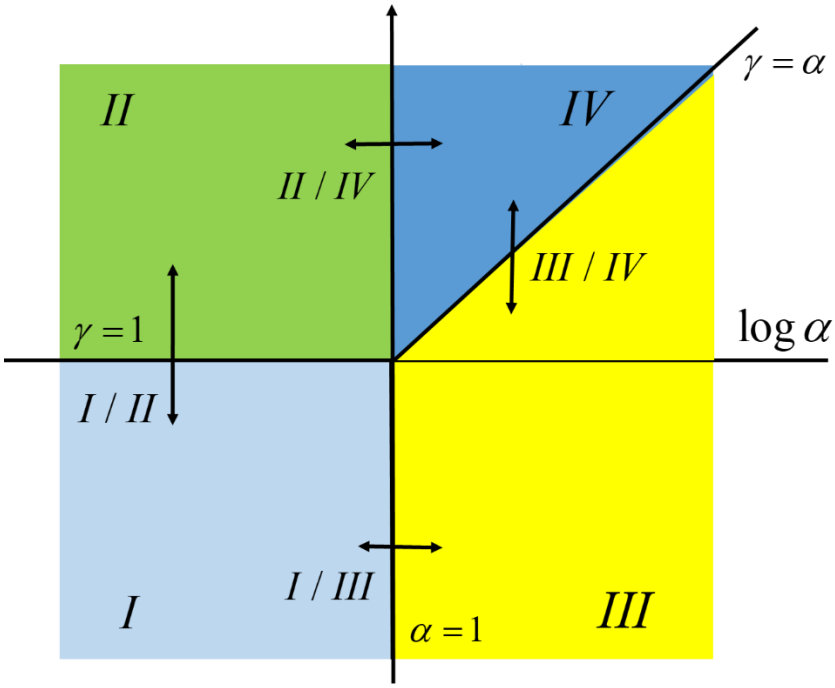

Figure 9. Kinetic case diagram illustrating the four kinetically limiting situations described in the text.

Here the current again is first order in substrate concentration, and half order with respect to enzyme concentration. Furthermore, the current is independent of layer thickness L and occurs in a thin reaction layer of thickness X_K . Note that eqn.33 joins the two cases I and II. When $\alpha >> 1$ then $s >> K_M$ and the catalytic kinetics are saturated. Hence the normalised current adopts the following form which is valid $\forall \gamma$:

$$y \cong \alpha \sqrt{\frac{\gamma}{\alpha}} \tanh\left[\sqrt{\frac{\gamma}{\alpha}}\right] \tag{38}$$

When γ is small then $\sqrt{\gamma/\alpha} << 1$ and $\tanh\left[\sqrt{\gamma/\alpha}\right] \cong \sqrt{\gamma/\alpha}$ and so the normalised current reduces to:

$$y \cong \gamma \tag{39}$$

This expression defines case III. Here the catalytic kinetics are more sluggish than substrate diffusion and the substrate concentration is the film is larger than the Michaelis constant for the catalytic reaction. Hence the current response for case III is:

$$i = nFAk_c e_\Sigma L \tag{40}$$

Hence the rate determining step involves the decomposition of the catalyst/substrate adduct to form products. This occurs throughout the entire thickness of the immobilized film. The current is zero order in substrate concentration and first order with respect to catalyst and layer thickness. Finally when $\gamma >> 1$ and the catalytic kinetics are rapid then eqn. 38 reduces to:

$$y \cong \sqrt{\alpha\gamma} \tag{41}$$

This defines case IV where both the catalytic kinetics are rapid and the substrate concentration in the layer is larger than the Michaelis constant. Under these circumstances the current response is given by:

$$i = nFA\left(k_c / \sqrt{K_M}\right) c_\Sigma X_K \sqrt{\kappa s^\infty} = nFA\sqrt{k_c \kappa D_S} e_\Sigma^{1/2} s^{\infty 1/2} \quad (42)$$

In case IV the current is half order with respect to substrate concentration in the layer, is half order with respect to enzyme loading and occurs in a thin reaction layer adjacent to the film/solution interface. Hence cases II and IV are connected via the following expression:

$$y \cong \alpha \sqrt{\frac{\gamma}{1+\alpha}} \quad (43)$$

This expression is obtained from eqn.26 by assuming $\sqrt{\gamma/1+\alpha}$ is large and so we note that $\tanh\left[\sqrt{\gamma/1+\alpha}\right] \cong 1$. In the kinetic case diagram cases II and IV are separated by the line $\gamma = \alpha$ located in the top right hand quadrant. Case IV pertains when one has thick catalytic layers and when the kinetics are saturated when s >> K_M. Under such circumstances one may expect that the outermost regions of the film will be completely saturated whereas the inner regions of the film are unsaturated.

Table 1. Limiting kinetic cases.

Case	Normalised current	Steady state current
I	$y = \alpha\gamma$	$i = nFA\left(k_c / K_M\right) e_\Sigma L \kappa s^\infty$
II	$y = \alpha\sqrt{\gamma}$	$i = nFA\sqrt{\left(k_c / K_M\right) e_\Sigma D_S} \kappa s^\infty$
III	$y = \gamma$	$i = nFAk_c e_\Sigma L$
IV	$y = \sqrt{\alpha\gamma}$	$i = nFA\sqrt{k_c e_\Sigma D_S \kappa s^\infty}$
V	$y = \frac{\alpha\gamma}{\beta}$	$i = nFA\left(k_c / K_M\right) e_\Sigma L K_I w^{-1} \kappa s^\infty$
VI	$y = \alpha\sqrt{\frac{\gamma}{\beta}}$	$i = nFA\sqrt{\frac{k_c e_\Sigma D_S K_I}{K_M w}} \kappa s^\infty$
VII	$y = \frac{\gamma}{\beta}$	$i = nFAk_c e_\Sigma L K_I w^{-1}$
VIII	$y = \sqrt{\frac{\alpha\gamma}{\beta}}$	$i = nFA\sqrt{\frac{k_c e_\Sigma D_S K_I \kappa s^\infty}{w}}$
IX	$y = \frac{\gamma}{\beta'}$	$i = nFAk_c e_\Sigma K_I' w^{-1} \kappa s^\infty$
X	$y = \sqrt{\frac{\alpha\gamma}{\beta'}}$	$i = nFA\sqrt{\frac{k_c e_\Sigma D_S K_I' \kappa s^\infty}{w}}$

When the kinetics are sluggish then γ is small then $\tanh\left[\sqrt{\frac{\gamma}{1+\alpha}}\right] \cong \sqrt{\gamma/(1+\alpha)}$ and $\forall\alpha$ the general eqn.26 reduces to:

$$y \cong \frac{\alpha\gamma}{1+\alpha} \quad (44)$$

This expression can be seen to join cases I and III. This is just a normalised form of the Michaelis Menten equation. It will be valid for thin films where there is very little concentration polarization of the substrate in the film and where the reaction kinetics are rate determining. We present a summary of the key kinetic cases and equations in table 1 and a reaction order summary in table 2.

Table 2. Diagnostic Reaction orders.

Case	s^{∞}	L	e_{Σ}	w
I	1	1	1	0
II	1	0	1/2	0
III	0	1	1	0
IV	1/2	0	1/2	0
V	1	1	1	-1
VI	1	0	1/2	-1/2
VII	0	1	1	-1
VIII	1/2	0	1/2	-1/2
IX	0	1	1	-1
X	1/2	0	1/2	-1/2

We note that the Albery equation presented in eqn.25 reproduces the limiting kinetic case expressions for the normalised current for cases I, II and III. However for case IV corresponding to $\alpha >> 1, 0 < \gamma < 2\alpha$, the limiting current is predicted to be :

$$y_A \cong \sqrt{2\alpha\gamma} \tag{45}$$

Hence we see that the expression for the normalised current response in these circumstances is $y \cong y_A / \sqrt{2}$ or approximately 0.71 times that predicted by the Albery model.

Now eqn.32 obtained via direct integration of the reaction/diffusion equation joins cases II and IV. We note that when $\alpha << 1$, then $\ln(1+\alpha) \cong \alpha - \alpha^2/2$ and $\alpha - \ln(1+\alpha) \cong \alpha^2/2$ and the normalised current reduces to $y \cong \alpha\sqrt{\gamma}$ which is case II. Alternatively, when $\alpha >> 1$ then $\alpha >> \ln\alpha$ and the normalised current reduces to $y \cong \sqrt{2\alpha\gamma}$ which is case IV and is the same as eqn.38. Hence case IV will be bounded by $1 < \alpha < \gamma/2$ rather than $1 < \alpha < \gamma$ as is predicted in our current approach. The governing expression for the steady state normalised current and the four kinetic sub cases are presented schematically in fig.10 below. Also included in this figure are the normalised current expressions joining the limiting kinetic cases.

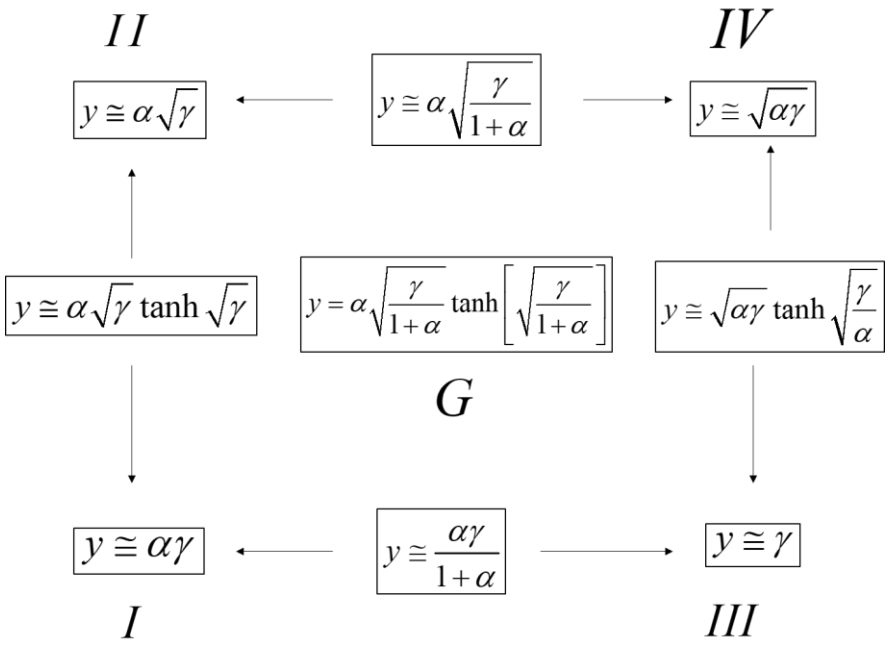

Figure 10. Schematic representation of the relation between the general expression for the normalised limiting current and the four sub cases I-IV. Also included are the expressions joining the limiting subcases.

We note that the limiting expressions for the normalised current can be used with experimental data to identify a particular rate limiting case.

2.2. Mixed Inhibition Effects Operative.

2.2.1. General Formulation Of The Problem

We now consider the more complicated situation where product formation at the enzyme molecule is affected by the presence of an inhibitor species I. The effect of substrate inhibition on the amperometric current response has been reported by Kulys and Baronas[21] and by Rajendran et al[22]. The former utilized a digital simulation to obtain the predicted current response whereas the latter utilized the Adomian Decomposition Method (ADM) to obtain the steady state amperometric current response. In the present communication we discuss the general situation of enzymatic biocatalysis exhibiting mixed inhibition according to the reaction scheme outlined below.

$$\begin{aligned} &S+E \underset{}{\overset{K_M}{\rightleftarrows}} ES \xrightarrow{k_c} P+E \\ &S+I \underset{K_I}{\rightleftarrows} EI \\ &ES+I \underset{K_I'}{\rightleftarrows} ESI \end{aligned} \qquad (46)$$

Note that in noncompetitive inhibition the inhibitor binds to a site that is different from the substrate binding site. In mixed inhibition, the inhibitor also binds the enzyme at a site other than the active site, and, as with non competitive inhibition may bind whether or not substrate is already bound

at the active site. We introduce the following dissociation constants (both having unity of mol cm^{-3}) of EI and ESI as follows:

$$K_I = \frac{[E][I]}{[EI]}$$
$$K_I' = \frac{[ES][I]}{[ESI]} \quad (47)$$

And we also note that $K_M \cong k'/k$ since we assume that $k_c << k'$. It is well established using the steady state approximation that the rate of product formation is given by the following expression:

$$R = \frac{\mathrm{d}p}{\mathrm{d}t} = \frac{k_c e_\Sigma s}{K_M\left(1+\frac{w}{K_I}\right)+s\left(1+\frac{w}{K_I'}\right)} \quad (48)$$

Here w denotes the inhibitor concentration. In scheme I we indicate the form that the rate equation takes under various types of inhibition. We note that eqn.41 defines the most general situation when $K_I = K_I'$. Here we have non competitive inhibition. In contrast when $K_I << K_I'$ we get competitive inhibition and the pertinent rate equation is given by:

$$R = \frac{dp}{dt} = \frac{k_c e_\Sigma s}{K_M\left(1+\frac{w}{K_I}\right)+s} \quad (49)$$

Clearly this pertains when $w/K_I' << 1$. On the other hand when $K_I >> K_I'$ then we obtain the uncompetitive limit with a characteristic rate expression given by:

$$R = \frac{dp}{dt} = \frac{\frac{k_c e_\Sigma s}{\left(1+\frac{w}{K_I'}\right)}}{\frac{K_M}{\left(1+\frac{w}{K_I'}\right)}+s} \quad (50)$$

In a thin conductive polymer film the pertinent reaction/diffusion equation when we adopt the general inhibition expression presented in eqn.41 is given by:

$$D_S\frac{\mathrm{d}^2 s}{\mathrm{d}x^2} - \frac{k_c e_\Sigma s}{K_M\left(1+\frac{w}{K_I}\right)+s\left(1+\frac{w}{K_I'}\right)} = 0 \quad (51)$$

Hence we see that for mixed inhibition both the substrate concentration and the Michaelis constant K_M are affected by the mediator concentration w . Note that we assume that the diffusion of the inhibitor within the film can be neglected.

We again introduce the following normalised variables:

$$\chi = \frac{x}{L} \quad \alpha = \frac{\kappa s^\infty}{K_M} \quad u = \frac{s}{\kappa s^\infty} \quad \gamma = \frac{k_c e_\Sigma L^2}{K_M D_S} \quad \omega = \frac{w}{\kappa s^\infty}$$
$$\lambda = \frac{\kappa s^\infty}{K_I} \quad \lambda' = \frac{\kappa s^\infty}{K_I'} \quad \beta = \lambda\omega = \frac{w}{K_I} \quad \beta' = \frac{w}{K_I'} = \lambda'\omega \quad (52)$$

In the latter expression ω denotes the normalised inhibitor concentration in the film, and β, β' compare the inhibitor concentration in the film with the respective dissociation constant values for EI and ESI respectively as outlined in eqn.47, whereas λ, λ' are parameters which compare the bulk concentration of the substrate in the film with the respective dissociation constants of the same inhibitor complexes.

It can be readily shown that the reaction/diffusion equation reduces to:

$$\frac{d^2u}{d\chi^2} - \frac{\gamma u}{1+\lambda\omega+(1+\lambda'\omega)\alpha u} = 0 \tag{53}$$

This can be written in an alternative manner as follows:

$$\frac{d^2u}{d\chi^2} - \frac{\gamma u}{1+\beta+\alpha(1+\beta')u} = 0 \tag{54}$$

This equation is subject to the following boundary conditions: $\chi = 0 \quad du/d\chi = 0 \quad u = u_0$, and when $\chi = 1, \quad u = u_1 = 1$ and so we again assume that concentration polarization of substrate in the solution can be neglected and that the film is electronically conducting. As before we can assume a general solution of eqn.47 of the following form:

$$u = A\cosh[\theta\chi] + B\sinh[\theta\chi] \tag{55}$$

From the boundary conditions we arrive at the following result for the concentration distribution of substrate in the thin film:

$$u(\chi) = \operatorname{sech}\theta\cosh[\theta\chi] = u_0\cosh[\theta\chi] \tag{56}$$

Also we note that

$$\left(\frac{du}{d\chi}\right)_1 = \theta\operatorname{sech}\theta\sinh\theta = \theta\tanh\theta \tag{57}$$

Hence the normalised current response under steady state conditions is given by:

$$y = \frac{iL}{nFAK_{\partial M}D_S} = \alpha\left(\frac{du}{d\chi}\right)_1 = \alpha\theta\tanh\theta \tag{58}$$

Following the AGM as outlined in the previous section we can readily show that:

$$\theta = \sqrt{\frac{\gamma}{1+\alpha+\lambda\left\{1+\frac{\alpha\lambda'}{\lambda}\right\}\omega}} = \sqrt{\frac{\gamma}{1+\alpha+\beta\left\{1+\frac{\alpha\beta'}{\beta}\right\}}} \tag{59}$$

Hence the concentration profile of substrate in the film is given by:

$$u(\chi) = u_0\cosh\left[\sqrt{\frac{\gamma}{1+\alpha+\beta\left\{1+\frac{\alpha\beta'}{\beta}\right\}}}\right] \tag{60}$$

Where we note that the substrate concentration at the support electrode surface is given by:

$$u_0 = \operatorname{sech}\theta = \operatorname{sech}\left[\sqrt{\frac{\gamma}{1+\alpha+\beta\left(1+\frac{\alpha\beta'}{\beta}\right)}}\right] \tag{61}$$

The substrate concentration distribution within the conductive layer defined by eqn. 60 with the value of u_0 the substrate concentration at the support electrode surface defined by eqn.61 is outlined in figure 11. In these calculations the reaction/diffusion parameter was fixed at $\gamma = 20$ and a range of values of the non-competitive inhibition factors were adopted (0,0.5, 1, 5 and 10) such that $\beta = \beta'$. These calculations were run for three characteristic levels of substrate concentration with $\alpha = 0.1, \alpha = 1, \alpha = 10$ respectively (fig.11A,B and C). We note the very marked effect of inhibition: the value of substrate concentration at the electrode surfaces increases significantly as the degree of inhibition increases for any value of the saturation parameter ranging from unsaturation to complete saturation. In these calculations a reasonable large value of the reaction/diffusion parameter was adopted corresponding to rapid substrate diffusion compared with substrate/enzyme reaction.

Furthermore, we can show that the normalised current is given by the following expression:

$$y = \alpha \sqrt{\frac{\gamma}{1+\alpha\left\{1+\frac{\beta}{\alpha}+\beta'\right\}}} \tanh\left[\sqrt{\frac{\gamma}{1+\alpha\left\{1+\frac{\beta}{\alpha}+\beta'\right\}}}\right] \qquad (62)$$

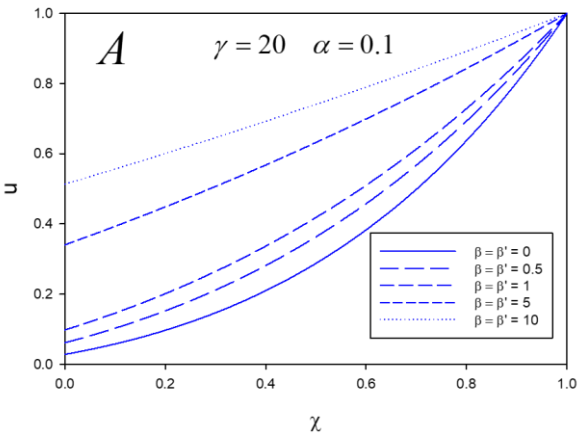

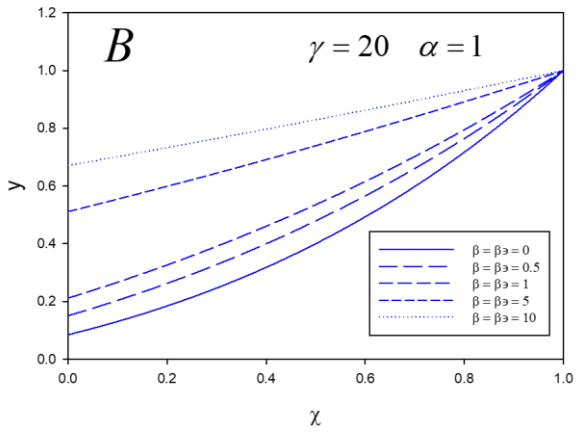

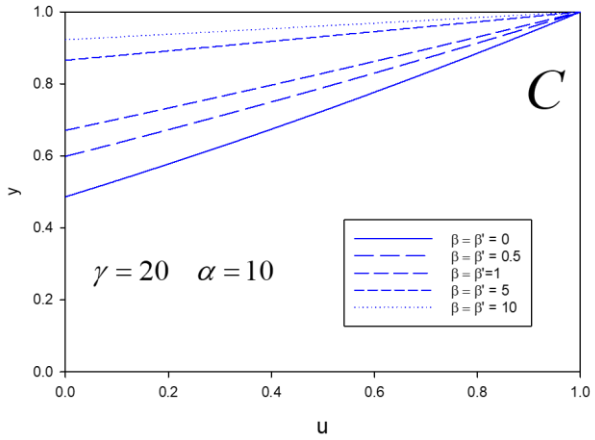

Figure 11. Substrate concentration profiles computed using eqn. 60 illustrating the effects of mixed inhibition on the substrate distribution profiles in the film. Substrate diffusion is significant. Panel A illustrates substrate/enzyme kinetics unsaturated where $\alpha << 1$. In panel B $\alpha = 1$, and in panel C the reaction kinetics are saturated with $\alpha >> 1$.

This is the general solution for the normalised current when non- competitive inhibition pertains. It should reduce to the less general forms of inhibition in the appropriate limit.

For instance when $\alpha\beta'/\beta << 1$ so $\alpha << \beta/\beta'$ which implies that $\alpha\left(1/K_I'\right) << 1/K_I$ which suggests that the formation of the ESI complex is not as favoured as EI complex formation . Under these circumstances eqn.62 reduces to:

$$y = \alpha\sqrt{\frac{\gamma}{1+\alpha+\beta}}\tanh\left[\sqrt{\frac{\gamma}{1+\alpha+\beta}}\right] \tag{63}$$

This expression describes the steady state normalised current response for competitive inhibition (the latter being described by the parameter $\beta = \lambda\omega$. On the other hand if $\alpha\beta'/\beta >> 1$ then eqn.62 reduces to:

$$y \cong \alpha\sqrt{\frac{\gamma}{1+\alpha\left(1+\beta'\right)}}\tanh\left[\sqrt{\frac{\gamma}{1+\alpha\left(1+\beta'\right)}}\right] \tag{64}$$

This describes uncompetitive inhibition. Furthermore, if $\beta = \beta'$ then eqn.62 reduces to:

$$y \cong \alpha\sqrt{\frac{\gamma}{1+\alpha\left(1+\beta+\frac{\beta}{\alpha}\right)}}\tanh\left[\sqrt{\frac{\gamma}{1+\alpha\left(1+\beta+\frac{\beta}{\alpha}\right)}}\right] \tag{65}$$

$$\cong \alpha\sqrt{\frac{\gamma}{(1+\alpha)(1+\beta)}}\tanh\left[\sqrt{\frac{\gamma}{(1+\alpha)(1+\beta)}}\right]$$

This is the desired current response for non-competitive inhibition under steady state conditions where substrate diffusion is taken into consideration.

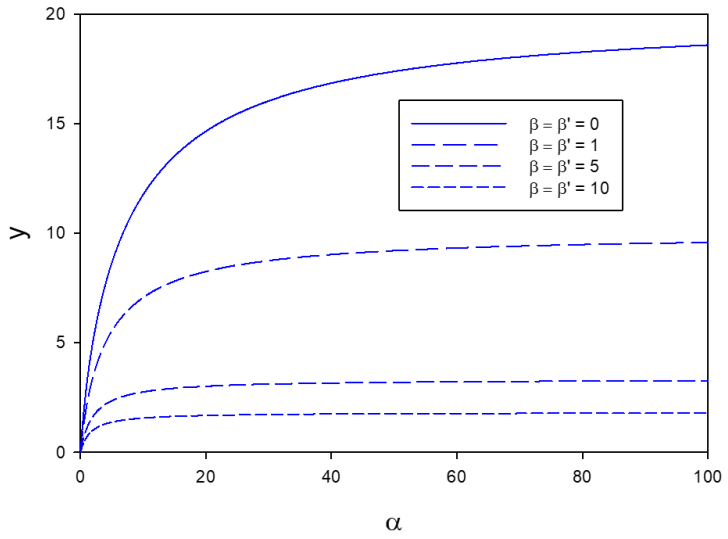

Figure 12. Variation of the normalised current y with saturation parameter. The curves were computed using eqn.65 at a fixed value $\gamma = 20$ using eqn.65 for the inhibition factor values indicated.

In figure 12 the normalised current response for non-competitive inhibition is presented. The contrast with the simple Michaelis-Menten response in the absence of inhibition is quite clear. The transition between linear unsaturated kinetics and the zero order unsaturated region becomes manifest at lower saturation parameter values as the extent of inhibition increases. Furthermore the steady state plateau current response decreases significantly as the level of inhibition increases.

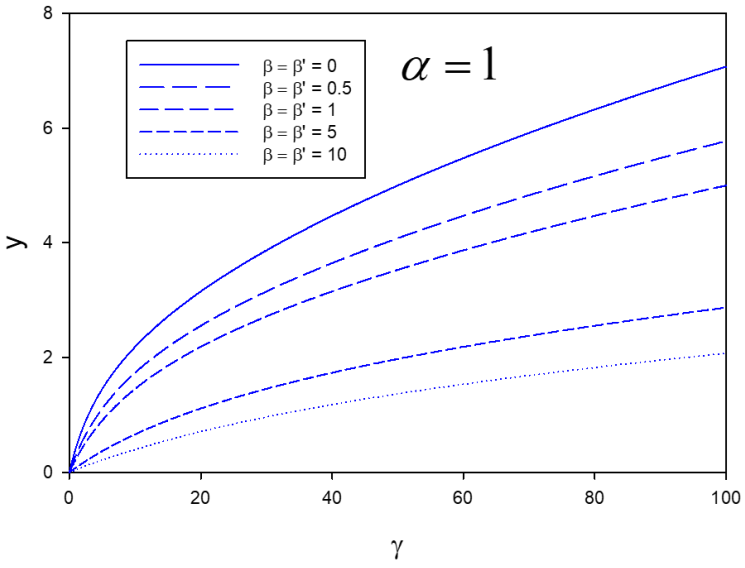

Figure 13. The variation of normalised current response with reaction/diffusion parameter for a saturation parameter $\alpha = 1$. The curves are computed using eqn.65 using the inhibition factor values indicated.

In figure 13 the variation of normalised current with the reaction/diffusion rate ratio is outlined. The curves in both the absence and presence of inhibition are compared. Inhibition clearly depresses the normalised current response for a fixed γ value. The calculations presented in fig.13 were performed

by assuming that $\alpha = 1$ which is just at the border between unsaturated and saturated kinetics. Similar profiles were derived for pure unsaturated kinetic conditions where $\alpha = 0.1$, and saturated kinetic conditions where $\alpha = 10$. The general shape of the response curves were similar to those outlined in fig.13.

2.2.2. Limiting Kinetic Cases.

From these general expressions we may readily derive 10 limiting cases. Turning to eqn.62 when $\gamma << 1 + \alpha + \beta\left(1 + \alpha\beta'/\beta\right)$ then

$$y \cong \alpha\theta^2 = \frac{\alpha\gamma}{1 + \alpha + \beta\left(1 + \alpha\beta'/\beta\right)} \tag{66}$$

This general expression produces four cases, and is identical to the expression obtained by invoking the thin film approximation where substrate diffusion effects through the film are ignored by setting $u \cong 1$ in the governing reaction/diffusion expression. We initially assume that $\alpha\beta'/\beta << 1$ in the denominator of eqn.66 then eqn.66 reduces to:

$$y \cong \frac{\alpha\gamma}{1 + \alpha + \beta} = \frac{\alpha\gamma}{1 + \alpha\left(1 + \beta/\alpha\right)} \tag{67}$$

Now when $\beta/\alpha << 1$ then eqn.67 reduces to eqn. 44 which describes the join between kinetic cases I and III in the absence of inhibition effects. Case I corresponds to the situation where $\alpha << 1$ and case III the converse, where $\alpha >> 1$, saturated enzyme/substrate kinetics are rate limiting, the normalised current $y \cong \gamma$ and the steady state current response is given by eqn.40. In contrast, when $\beta/\alpha >> 1$ where inhibition is important eqn.57 reduces to:

$$y \cong \frac{\alpha\gamma}{1 + \beta} \tag{68}$$

This expression pertains to competitive inhibition (CI). This defines a case I/V situation. When $\beta << 1$ and still $\beta >> \alpha$ eqn.68 reduces to case I discussed previously with $y \cong \alpha\gamma$, where the enzyme/substrate kinetics are unsaturated, and the current response is given by eqn.35. In contrast when competitive inhibition effects are significant and $\beta >> 1$, we obtain the case V scenario:

$$y \cong \frac{\alpha\gamma}{\beta} \tag{69}$$

Here the current response is given by:

$$i = nFA\frac{k_c e_\Sigma L K_I \kappa s^\infty}{K_M w} \tag{70}$$

For case V the enzyme/substrate kinetics are again unsaturated and inhibition is manifested by the inverse proportionality between inhibitor concentration w and current response. The reaction order is 1 with respect both to enzyme loading and layer thickness.

When $\alpha\beta'/\beta >> 1$ then eqn.59 reduces to:

$$y \cong \frac{\alpha\gamma}{1 + \alpha\left(1 + \beta'/\alpha\right)} \tag{71}$$

This expression pertains when inhibition is uncompetitive (UC). Again when $\beta'/\alpha << 1$ eqn.64 reduces to eqn.44 defining a I/III case. In contrast when $\beta' >> \alpha$ eqn.71 reduces to:

$$y \cong \frac{\alpha\gamma}{1+\alpha\beta'} \tag{72}$$

This expression joins cases I and IX. When $\alpha\beta' << 1$ uncompetitive inhibition effects can be disregarded and eqn.65 reduces to case I again. In contrast when $\alpha\beta' >> 1$ then we get case IX in which the normalised current is given by:

$$y \cong \frac{\gamma}{\beta'} \tag{73}$$

Hence the net current response is

$$i = \frac{nFAk_c e_\Sigma LK_I'}{w} \tag{74}$$

Here the enzyme/substrate kinetics are saturated and the current is zero order in substrate concentration. The current is first order with respect to enzyme loading and layer thickness, and inversely proportional to inhibitor concentration as we would expect.

All of the cases considered so far, I, II, V and IX correspond to the situation where the concentration profile throughout the layer is uniform or nearly so. Diffusion will be fast and reaction kinetics slow and rate determining. Under such circumstances reaction occurs throughout the entire film of thickness L. We now turn to the opposite situation when reaction kinetics are facile. This will be the case when $\gamma >> 1+\alpha+\beta\left(1+\alpha\beta'/\beta\right)$. Here we get:

$$y \cong \alpha\theta = \alpha\sqrt{\frac{\gamma}{1+\alpha+\beta\left(1+\alpha\beta'/\beta\right)}} \tag{75}$$

Again we can identify some limiting kinetic cases. We assume $\alpha\beta'/\beta << 1$ which suggests competitive inhibition and so the normalised current response reduces to:

$$y \cong \alpha\sqrt{\frac{\gamma}{1+\alpha\left(1+\beta/\alpha\right)}} \tag{76}$$

If we can neglect competitive inhibition then $\beta/\alpha << 1$ and we obtain eqn.43 again which describes the join between cases II and IV. When $\alpha << 1$ we get $y \cong \alpha\sqrt{\gamma}$ and the current response is given by eqn.37. Here the current is first order in substrate concentration, half order in enzyme loading, and is independent of the layer thickness. In contrast case IV pertains with $y \cong \sqrt{\alpha\gamma}$ when $\alpha >> 1$ and the current response is described by eqn.42, where the reaction order is half order with respect to enzyme loading and substrate concentration. Again the current is independent of layer thickness. Conversely, when $\beta/\alpha >> 1$ then competitive inhibition effects are operating and eqn.76 reduces to:

$$y \cong \alpha\sqrt{\frac{\gamma}{1+\beta}} \tag{77}$$

This expression defines the join between cases II and VI. When $\beta << 1$ we again get case II. When $\beta >> 1$ the normalised current reduces to

$$y \cong \alpha\sqrt{\frac{\gamma}{\beta}} \tag{78}$$

This defines case VI. The current response under these conditions is given by:

$$i = nFA\sqrt{\frac{k_c D_S e_\Sigma K_I}{K_M w}}\kappa s^\infty \tag{79}$$

Hence the reaction order is first order with respect to substrate concentration, half order with respect to enzyme loading and negative half order with respect to inhibitor concentration., and zero order with respect to layer thickness. Hence the enzyme substrate kinetics are unsaturated and occur within a thin reaction layer located within a zone adjacent to the film/solution interface.

Returning to eqn.75 we focus attention on the case where $\alpha\beta'/\beta >> 1$. This corresponds to the situation where competition is uncompetitive. Hence eqn.75 reduces to:

$$y \cong \alpha\sqrt{\frac{\gamma}{1+\alpha\beta'}} \tag{80}$$

This expression defines the join between cases II and X. When $\alpha\beta' << 1$ uncompetitive inhibition is not an issue and we obtain case II described previously for ordinary Michaelis Menten kinetics. In contrast when $\alpha\beta' >> 1$ then case X pertains and the normalised flux is given by:

$$y \cong \sqrt{\frac{\alpha\gamma}{\beta'}} \tag{81}$$

In this case the current response is given by:

$$i = nFA\sqrt{\frac{k_c D_S e_\Sigma K_I' \kappa s^\infty}{w}} \tag{82}$$

Here the reaction kinetics are half order with respect to enzyme loading and substrate concentration, are zero order with respect to layer thickness and inverse half order with respect to inhibitor concentration.

Finally we look at non-competitive inhibition where $\beta = \beta'$ and the expression for the normalised current is given by eqn.65. When $\gamma < (1+\alpha)(1+\beta)$ we obtain:

$$y = \frac{\alpha\gamma}{(1+\alpha)(1+\beta)} \tag{83}$$

When $\beta << 1$ eqn.83 reduces to eqn.44 defining a join between cases I and III. In contrast when $\beta >> 1$ eqn.83 reduces to:

$$y \cong \frac{\alpha\gamma}{(1+\alpha)\beta} \tag{84}$$

This expression defines the join between cases V and VII. When $\alpha << 1$ we obtain eqn.69 again which defines case V. In contrast when $\alpha >> 1$ we get

$$y \cong \frac{\gamma}{\beta} \tag{85}$$

This defines case VII. Here the current response is given by:

$$i = \frac{nFAk_c e_\Sigma L K_I}{w} \tag{86}$$

Here the substrate kinetics are unsaturated and inhibition is operative. The reaction occurs throughout the entire layer. The kinetics are zero order in substrate, first order in enzyme loading, first order with respect to layer thickness and the rate is inversely proportional to the inhibitor concentration.

Finally when $\gamma >> (1+\alpha)(1+\beta)$ then we get:

$$y \cong \alpha \sqrt{\frac{\gamma}{(1+\alpha)(1+\beta)}} \tag{87}$$

When $\beta << 1$ then eqn.87 reduces to eqn.43 outlined previously which joins cases II and IV. When $\beta >> 1$ we get

$$y \cong \alpha \sqrt{\frac{\gamma}{(1+\alpha)\beta}} \tag{88}$$

This expression joins cases VI and VIII when non competitive inhibition operates. When $\alpha << 1$ we get

$$y \cong \alpha \sqrt{\frac{\gamma}{\beta}} \tag{89}$$

This defines case VI. In this situation the current response is given by:

$$i = nFA \sqrt{\frac{k_c e_\Sigma D_S K_I}{K_M w}} \kappa s^\infty \tag{90}$$

Here the enzyme/substrate kinetics are unsaturated and non competitive inhibition operates. The reaction takes place in a thin reaction layer. The kinetics are first order in substrate concentration and half order in enzyme concentration. The kinetics are zero order in layer thickness and are negative first order with respect to inhibitor concentration. In contrast when $\alpha >> 1$ we get case VIII and note that:

$$y \cong \sqrt{\frac{\alpha\gamma}{\beta}} \tag{91}$$

Here the current response is given by:

$$i = nFA \sqrt{\frac{D_S k_c e_\Sigma K_I \kappa s^\infty}{w}} \tag{92}$$

In case VIII the enzyme/substrate kinetics are saturated. Non competitive inhibition operates. The reaction rate is independent of substrate concentration, is negative half order with respect to inhibitor concentration , is independent of layer thickness and is half order with respect to enzyme loading. In conclusion we note that non-competitive inhibition is associated with 8 cases: I, II, III, IV, V, Vi, VII and VIII. Competitive inhibition is associated with 6, namely I,II,III,IV,V, VI. Uncompetitive inhibition is also associated with 6 cases namely I,II,III,IV,IX,X. We gather together all of the 10 limiting cases developed in the paper in Table 1, and in table 2 diagnostic reaction orders with respect to substrate concentration, enzyme loading, layer thickness and inhibitor concentration are presented. Determination of these quantities will enable case identification to be established using experimental data.

In figure 14 we illustrate the interconnection between the expressions derived for the limiting current response when the different inhibition models operate.

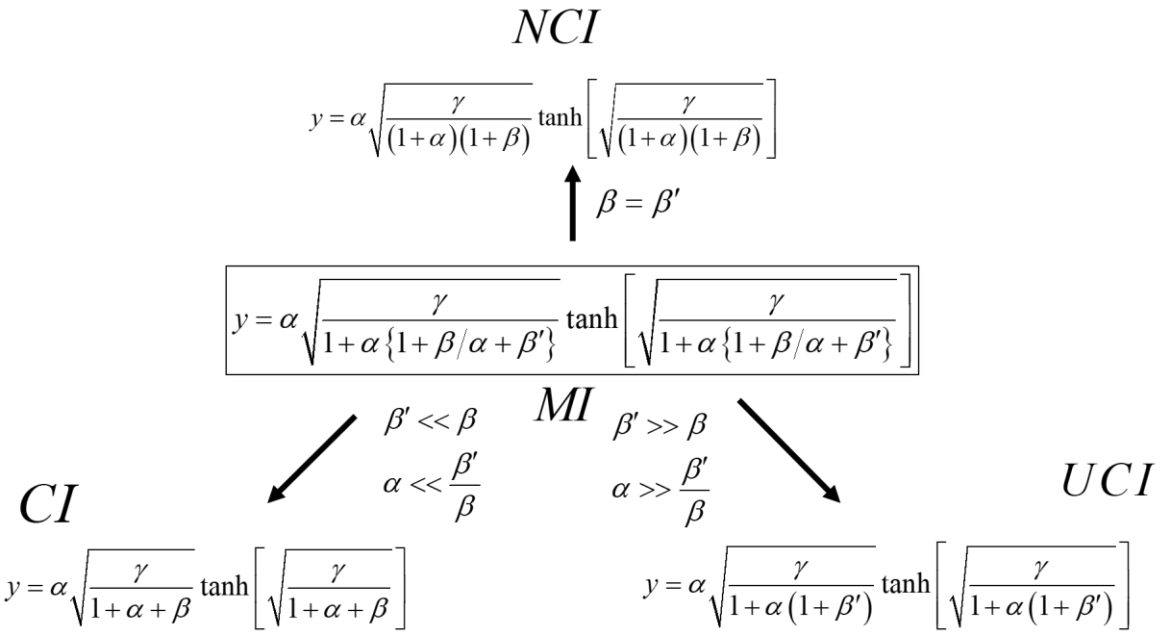

Figure 14. Schematic representation of the characteristic normalised current response for the various inhibition types.

In the analysis presented in this paper we have neglected the effect of concentration polarization in the solution. This can, of course be ensured experimentally by using the rotating disc electrode and by extrapolating the current data to infinite rotation speed. This is done using the well established Koutecky Levich plot in which inverse current is plotted as a function of inverse square root of rotation speed as follows:

$$\frac{nFA}{i} = I_{KL} + S_{KL}\omega^{-1/2} \tag{93}$$

The Koutecky –Levich intercept is given by the inverse reaction flux corrected for the effect of mass transport in the external solution :

$$I_{KL} = \frac{1}{f_K} \tag{94}$$

Whereas the Koutecky-Levich slope is given by

$$S_{KL} = 1.55 D_S'^{2/3} \nu^{-1/6} s^{\infty} \tag{95}$$

In the latter expression ν represents the kinematic viscosity of the solution and D_S' denotes the diffusion coefficient of the substrate in the solution as opposed to that in the layer. The mass transport corrected kinetic flux is directly related to the various limiting expressions presented in table 1 for the steady state current by noting that

$$f_{K,\omega\to\infty} = \frac{i}{nFA} \tag{96}$$

This procedure has been previously discussed by Lyons[1,2].

2.2.3. The Thin Layer Approximation (Tla).

We finally focus attention of the Thin Layer Approximation where it is assumed that diffusion of substrate through the layer is not rate limiting. This corresponds to a pure kinetic situation. Reaction occurs uniformly throughout the thin film and we can assume that the substrate concentration profile is uniform throughout the layer and is given by $u \cong 1$. Under such circumstances eqn.54 reduces to:

$$\frac{d^2u}{d\chi^2} - \frac{\gamma}{1+\beta+\alpha(1+\beta')} = 0 \qquad (97)$$

This equation is subject to the following boundary conditions: $\chi = 0 \quad du/d\chi = 0 \quad u = u_0$, and when $\chi = 1, \quad u = u_1 = 1$. A first integration affords:

$$\frac{du}{d\chi} = \frac{\gamma}{1+\alpha\{1+\beta/\alpha+\beta'\}}\chi + A \qquad (98)$$

Whereas a second integration yields:

$$u = \frac{\gamma}{2\{1+\alpha(1+\beta/\alpha+\beta')\}}\chi^2 + A\chi + B \qquad (99)$$

We may readily show that : $A = 0$ and $B = 1 - \frac{\gamma}{2\{1+\alpha(1+\beta/\alpha+\beta')\}}$ and note that the concentration profile of substrate is given by:

$$u(\chi) \cong 1 - \frac{\gamma}{2\{1+\alpha(1+\beta/\alpha+\beta')\}}\{1-\chi^2\} \qquad (100)$$

Furthermore the normalised current response is given by:

$$y = \alpha\left(\frac{du}{d\chi}\right)_1 = \frac{\alpha\gamma}{1+\alpha\{1+\beta/\alpha+\beta'\}} \qquad (101)$$

One can readily show that the following general relationship pertains:

$$\frac{nFA}{i} = \left\{\frac{1}{(k_c/K_M)c_\Sigma L}\left(1+\frac{w}{K_I}\right)+\frac{w}{K_I'}\frac{1}{D_s/L}\right\}\frac{1}{\kappa s^\infty}+\frac{1}{k_c e_\Sigma L} \qquad (102)$$

Hence we predict that for general inhibition in a thin film under pure kinetic conditions where substrate diffusion is fast a plot of nFA/i vs substrate concentration is linear with an intercept given by:

$$I_{TFA} = \frac{1}{k_c e_\Sigma L} \qquad (103)$$

And slope given by:

$$S_{TFA} = \frac{1}{\kappa(k_c/K_M)e_\Sigma L}\left(1+\frac{w}{K_I}\right)+\frac{w}{K_I'(\kappa D_S/L)} \qquad (104)$$

This depends on the inhibitor concentration w . When inhibition effects are absent eqn.102 immediately reduces to the well established Linewaver-Burk equation.

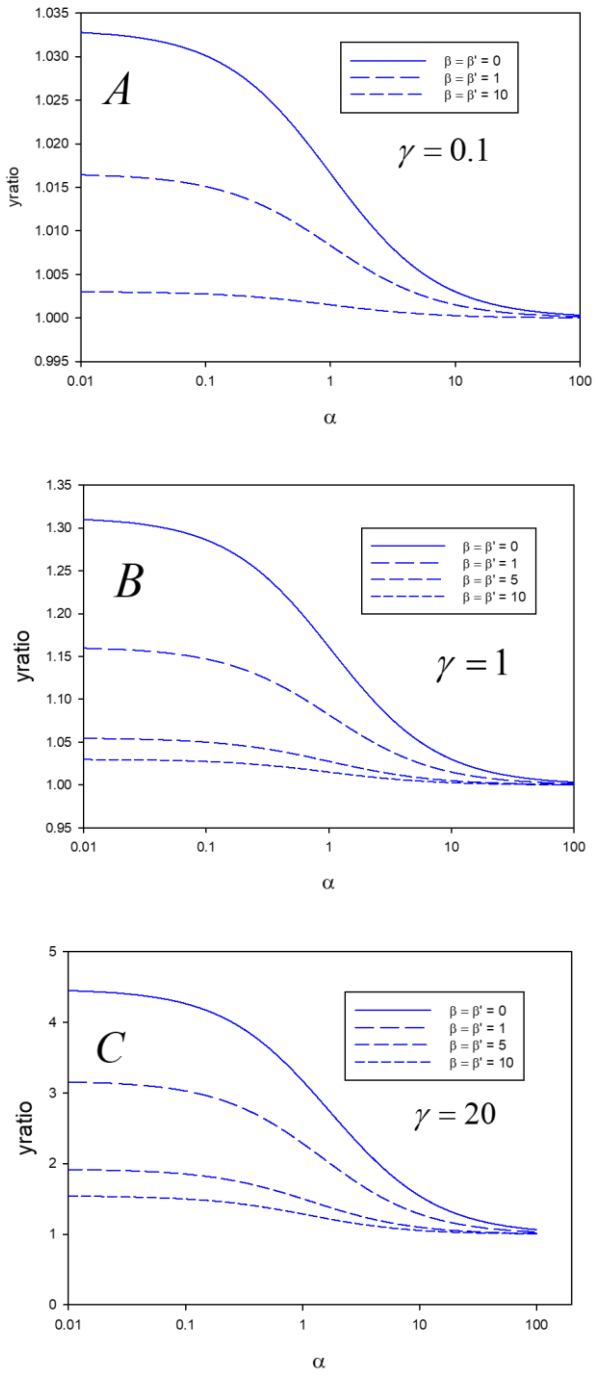

Figure 15. Computations outlining the regions of validity of the thin layer approximation corresponding to pure substrate/enzyme reaction kinetics.

Finally we can compare y with y_{TFA} and show that:

$$\frac{y_{TFA}}{y} = \sqrt{\frac{\gamma}{1+\alpha\{1+\beta/\alpha+\beta'\}}}\coth\left[\sqrt{\frac{\gamma}{1+\alpha\{1+\beta/\alpha+\beta'\}}}\right] \tag{105}$$

This expression is outlined in figure 15 where we have set the $\text{yratio} = y_{TLA}/y$. In these calculations we have computed this ratio, which quantifies how good the thin layer approximation is compared with the full expression for the normalised current, as a function of the saturation parameter for three different values of the reaction/diffusion parameter. In panel A $\gamma = 0.1$ and reaction is slower than substrate diffusion through the layer. Here we would expect that pure kinetics are rate determining and so the TLA should approximate well to the full expression derived. This is indeed the case as illustrated in figure 15A. The effect of inhibition is also apparent. When inhibitor concentration increases the ratio improves and is close to unity over a wide range of substrate concentration values. In panel B calculations are outlined, when diffusion and chemical reaction fluxes are equal. Good agreement between the thin film expression and the full expression is observed when the enzyme/substrate reaction kinetics are saturated, and when the substrate reaction kinetics are affected significantly by inhibition effects. Finally, in panel C we outline the situation where diffusion is significant and rate determining. Here the agreement between the two models is not at all good even when the substrate concentration in the film is significantly larger than the Michaelis constant of the enzyme/substrate reaction. Again, when inhibition effects are important the value of the current ratio is smaller over a large range of substrate concentrations.

4. CONCLUDING COMMENTS.

In this paper we have examined the problem of describing the transport and kinetics of catalytic reactions in a bounded region such as a conductive polymer modified electrode. The kinetics are modified Michaelis - Menten in type due to the presence of a generalised inhibition process. The relevant reaction/diffusion has been formulated and the AGM technique has been applied to obtain an analytical solution both of the substrate concentration profile within the film and the normalised amperometric current response which are valid over a large range of values of substrate concentration. This analytical solution for normalised current response has been used to derive 10 useful limiting kinetic equations which can be used in experimental studies and which convey useful physical insight into the underlying physical chemistry of the system. Further work is currently ongoing to extend the analysis to the examination of transient reaction/diffusion and to the examination of reaction/diffusion at polymer coated thin films deposited on inlaid micro-discs.

ACKNOWLEDGEMENTS.
The author is grateful to Trinity College Dublin and the School of Chemistry for providing funding.

References

1. MEG Lyons in Electroactive Polymer Electrochemistry : Fundamentals, MEG Lyons (Ed), Plenum Press, New York, 1994, Chapter 2, pp.237-374.
2. MEG Lyons in Polymeric Systems, Eds. I Prigogine and S Rice, *Adv. Chem. Phys.*, 96 (1996) 297-624.

3. (a) CP Andrieux, JM Dumas-Bouchiat, JM Saveant, *J. Electroanal. Chem*., 131 (1982) 1-35. (b) CP Andrieux, JM Saveant, *J. Electroanal. Chem*., 134 (1982) 163-166. (c) CP Andrieux, JM Saveant, *J. Electroanal. Chem*., 171 (1984), 65-93.
4. WJ Albery, AR Hillman, *J. Electroanal. Chem*., 170 (1984) 27-49.
5. C Costentin, JM Saveant, *J Phys. Chem.C.*, 119 (2015) 12174-12182.
6. C Costentin, JM Saveant, *ACS Catalysis*, 7 (2017), 4876-4880.
7. MEG Lyons, *Electroanalysis*, 27 (2015) 1-19.
8. MEG Lyons, JC Greer, CA Fitzgerald, TB Bannon, PN Bartlett, *Analyst*, 121 (1996) 715-731.
9. MEG Lyons, *Int. J. Electrochem. Sci*., 4 (2009) 1196-1236.
10. G Rahamathunissa, P. Manisankar, L. Rajendran, K. Venugopal, *J. Math Chem*., 49 (2011) 457-474.
11. G Rahamathunissa, L Rajendran, *J Math Chem*., 44 (2008) 849-861.
12. A Malvandi, DD Ganji, *J. Electroanal. Chem*., 711 (2013) 32-37.
13. A Shanmugarajan, S Alwarappan, S Somasundaram, R Lakshmanan, *Electrochim. Acta*, 56 (2011) 3345-3352.
14. A Meena L Rajendran, *J Electroanal. Chem*., 644 (2010) 50-59.
15. K Murali, B Sonaiyappan, R Lakshmanan, *Chem. Phys. Lett*., 715 (2019) 20-28.
16. KM Dharmalingam, M Veeramuni, *J Electroanal. Chem*., 844 (2019) 1-5.
17. MEG Lyons, *J. Solid State Electrochemistry*, 2020, in press.
18. WJ Albery, AEG Cass, ZX Shu, *Biosens. & Bioelectronics*, 5 (1990) 367-378.
19. L Ranjendran, S Anitha, *Electrochim Acta*, 102 (2013) 474-476.
20. JH He, LF Mo, *Electrochim. Acta*, 102 (2013)472-473.
21. J Kulys, R Baronas, *Sensors*, 6 (2006) 1513-1522.
22. P Manimozhi, A Subbiah, L Rajendran, *Sens.& Act.B: Chemical*, 147 (2010) 290-297.